Nanoscale Res Lett (2010) 5:823–828
DOI 10.1007/s11671-010-9568-3

NANO EXPRESS

Study on Growth Kinetics of CdSe Nanocrystals with a New Model

Huaipeng Su · John David Dixon · Andrew Y. Wang · Jeremy Low · Jian Xu · Jingkang Wang

Received: 4 November 2009 / Accepted: 24 February 2010 / Published online: 25 March 2010

Abstract A model which involves both bulk diffusion process and surface reaction process has been developed for describing the growth behaviour of nanoparticles. When the model is employed, hypothesising that either of the processes alone dominates the overall growth process is unnecessary. Conversely, the relative magnitude of contributions from both processes could be obtained from the model. Using this model in our system, the growth process of CdSe QDs demonstrated two different growth stages. During the first stage, the growth of CdSe QDs was dominated by bulk diffusion, whereas, neither the bulk diffusion process nor the surface reaction process could be neglected during the later stage. At last, we successfully modelled the Ostwald ripening of CdSe QDs with LSW theories.

Keywords Growth kinetics · Semiconductor nanocrystals · Model · CdSe · Ostwald ripening

Introduction

A lot of work has been devoted to the preparation of colloidal semiconductor nanocrystals, also called quantum dots (QDs), and the investigation of their optical properties and applications during the past decade. Highly monodisperse II–VI [1–4] and III–V [5–7] QDs have been prepared and applied in various applications, such as light-emitting diodes [8, 9], biological labels [10, 11], solar cells [12]. There have, however, been relatively few papers on the crystallization kinetics of QDs [13].

With a quantitative understanding of the kinetics during crystallization, crystal growth could be optimized by adjusting some experimental parameters, so that high-quality crystals are reproducibly prepared. Several methods have been developed to prepare high-quality CdSe QDs, which provides an ideal system to verify the kinetic model of particle growth in solution. If the level of solution supersaturation could be measured, experimental growth rates could then be easily correlated with the classic growth model. Unfortunately, in the case of CdSe QDs, the supersaturation is generally unable to be measured accurately. Nevertheless, Yu et al. [14] found that the extinction coefficient per mole of CdSe at the first excitonic absorption peak was depended strongly on the size, and not dependent on synthesis methods, surface ligands, etc. We used this method to assess the size and concentration of CdSe QDs from the peak position and absorbance contained within the absorption spectrum.

The crystallization kinetics of CdSe QDs has been reported in several papers. Peng et al. observed "focusing" and "defocusing" of size distribution during the growth of several II–VI and III–V QDs [15]. They explained the behaviour by a diffusion-controlled process. Xie et al. reported another diffusion-controlled growth model to study the crystallization kinetics of CdSe synthesized via the TOP–TOPO–HDA route [16]. Bullen and Mulvaney, on the other hand, suggested a surface reaction-controlled model to explain the growth behaviour [17].

H. Su · J. Wang (✉)
State Key Laboratory of Chemical Engineering, School of Chemical Engineering and Technology, Tianjin University, 300072 Tianjin, Peoples' Republic of China
e-mail: wangjkch@tju.edu.cn

J. D. Dixon · A. Y. Wang
Ocean NanoTech LLC, 2143 Worth Lane, Springdale, AR 72764, USA

J. Low · J. Xu
Department of Engineering Science and Mechanics, Penn State University, University Park, PA 16802, USA
e-mail: jianxu@engr.psu.edu

A colloidal particle grows by a sequence consisting of bulk diffusion of crystallizing materials towards the crystal surface and integration of crystallizing materials into the crystal lattice (also called surface reaction), so the growth of particles should be determined by both diffusion and reaction processes. The published investigations on growth kinetics of CdSe QDs, however, were almost based on the hypothesis that the growth rate was determined by either diffusion process or reaction process.

In this report, a new growth model that involves both crystallizing materials diffusion in bulk solution and surface reaction processes was developed and employed in the growth process of CdSe QDs. Instead of hypothesising, the possible growth determining process could be elucidated with the new model. At last we modelled the Ostwald ripening of CdSe QDs with LSW theories.

Experimental Section

Preparation of CdSe QDs

In a typical procedure, 0.0314 g of CdO, 0.1835 g of ODPA and 9.8 g of ODE were loaded into a 100-mL three-neck flask and heated to 310°C. The solution was cooled down to room temperature after becoming colourless. Then, 9.0 g of ODA and 1.5 g of TOPO were added into the solution and heated under nitrogen flow to 280°C, at which point 1.1 mL of Se/TBP (2.0 M) solution was swiftly injected into the reaction flask. The injection of Se stock solution resulted in immediate nucleation of CdSe QDs. The solution was cooled quickly to 230°C for the growth of CdSe QDs. Strong coordinating alkylphosphonic acid was used to prepare cadmium precursor in order to maintain control over the growth.

Samples were taken at various time intervals and diluted immediately with toluene to quench the QDs growth. The masses of the samples and toluene were precisely weighed in order to calculate the QDs concentration in the reaction solution. UV–vis absorption and photoluminescence (PL) spectra were collected on a Perkin Elmer Lambda 45 UV/vis spectrophotometer and a Fluoromax-3 spectrophotometer, respectively.

Simulation Model

As soon as nuclei are formed in a supersaturated solution, they begin to grow into crystals. Generally, two main processes occur sequentially during the growth of crystals from solution [18]: the mass transport of crystallizing materials from the bulk supersaturated solution to the crystal-solution interface by bulk diffusion and the incorporation of crystallizing materials into the crystal lattice through the surface reaction process.

We start with a model describing the growth behaviour of a spherical nanoparticle of radius r, as shown in Fig. 1.

For a diffusion layer of thickness δ, the total flux of solute (crystallizing materials), J, passing through a spherical surface with radius x can be derived by Fick's law as

$$J = 4\pi x^2 D\frac{\mathrm{d}C}{\mathrm{d}x} \tag{1}$$

where D is the diffusion coefficient and C is the solute concentration at x ($r \le x \le \delta$). Under steady-state growth conditions, integration of $C(x)$ from $r + \delta$ to r gives

$$J = \frac{4\pi Dr(r+\delta)}{\delta}(C_b - C_i) \tag{2}$$

where C_b is the bulk solute concentration and C_i is the solute concentration at the interface.

If the surface reaction process is first-order, which is a reasonable assumption for high supersaturation [18], the total flux of solute J, can be written as

$$J = 4\pi r^2 k(C_i - C_{eq}) \tag{3}$$

where k is the rate constant and C_{eq} is the equilibrium concentration of the particle of radius r.

On the other hand, from mass balance, J is related to $\mathrm{d}r/\mathrm{d}t$ as

$$J = \frac{4\pi r^2}{V_m}\frac{\mathrm{d}r}{\mathrm{d}t} \tag{4}$$

where V_m is the molar volume of the solid.

With Eqs. (2), (3) and (4), one obtains

$$\frac{\mathrm{d}r}{\mathrm{d}t} = \frac{DkV_m(r+\delta)}{D(r+\delta) + k\delta r}(C_b - C_{eq}) \tag{5}$$

For nanoparticles, the radius is small compared to the diffusion layer thickness ($r << \delta$), Eq. (5) can be reduced to

$$\frac{\mathrm{d}r}{\mathrm{d}t} = \frac{DkV_m}{D + kr}(C_b - C_{eq}) \tag{6}$$

We define a dimensionless variable $H = D/(kr)$ as a representative of the relative magnitude of contributions

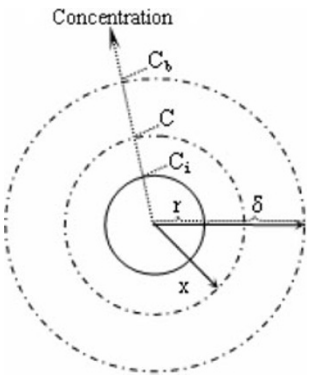

Fig. 1 The scheme of diffusion model of a spherical nanoparticle

from bulk diffusion and surface reaction. When $H >> 1$, the mass transport to the surface has a much higher rate than that of surface reaction, therefore the rate determining process is the surface reaction process. In this case, particle growth can be regarded as a surface reaction-controlled growth. Conversely, if $H << 1$, bulk diffusion process will be the rate determining process and particle growth can be regarded as a diffusion-controlled growth.

Results and Discussion

Figure 2 illustrates the temporal evolution of the particle size and concentration during the synthesis of CdSe QDs. After a burst nucleation, the concentration of CdSe QDs rapidly reached a "maximum" due to a prolonged formation of relatively small particles. As the supersaturation reduced resulting from the crystallizing materials in solution being consumed and a quick drop of temperature, the nucleation stopped, and the critical size of nuclei increased beginning the crystal growth process. At the very beginning of this process, some small particles dissolved due to the increased critical size resulting in a dramatic drop in the concentration of CdSe QDs and a quick increase in the QDs' size. Subsequently, although the concentration kept reducing and the size kept increasing, the range of change was small. At the same time, the absorption and PL spectra peaks became narrower (Fig. 3), which means there is a focusing of the size distribution [19]. The reaction then went into a relatively stable process during which the CdSe nanocrystal growth was slow, and both the concentration and average size remained almost constant. This can also be obtained from the corresponding absorption and PL spectra that showed a gradual broadening of the peaks, which meant that the size distribution broadened, whereas the peaks' positions did not change much (Fig. 3). The

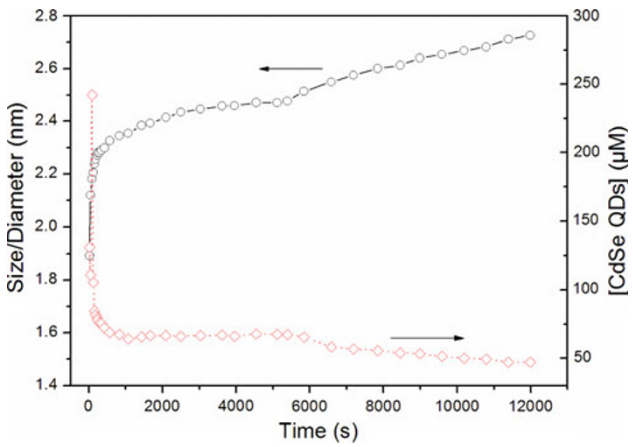

Fig. 2 Temporal evolution of the size (*black*) and concentration (*red*) of the CdSe QDs. (Color figure online)

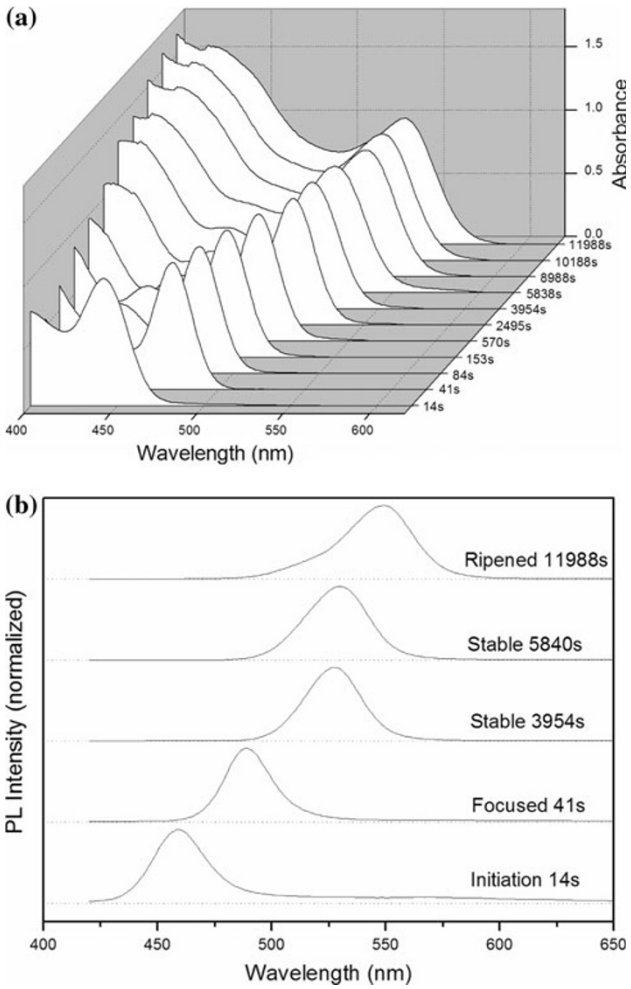

Fig. 3 Temporal evolution of UV–vis absorption (**a**) and PL (**b**) spectra of CdSe QDs during the synthesis

broadening of size distribution most likely resulted from the Gibbs–Thomson effect. This stage can be regarded as an "annealing" process of CdSe crystals. Although some broadening occurred in the last stage of the growth process, the size distribution of CdSe QDs stayed narrow. The PL FWHMs were under 30 nm during the overall growth process. Finally, when the supersaturation was depleted, Ostwald ripening occurred, during which large particles grew by means of sacrificing small ones. Hence, Ostwald ripening reduced the number of particles, increased the average size and broadened the size distribution of particles (Figs. 2 and 3). The PL spectra became asymmetric with an obvious tail in the short-wavelength region (Fig. 3b).

Nucleation took place so rapidly that it is very difficult to study the nucleation kinetics. From the aforementioned discussion, however, we know that the nucleation and the subsequent processes (viz. growth process and Ostwald ripening) were well separated. Thereby, we have simulated only the kinetics of growth and Ostwald ripening.

Growth Process

The TEM image (Fig. 4) indicates the as-prepared CdSe particles are dot shaped, so it is reasonable to use the model described previously to simulate the growth process. In order to simulate the kinetics of CdSe QDs crystallization, we need the solute concentration in solution. Under steady-state growth conditions, the concentration of crystals without nucleation and conglomeration should theoretically remain constant during the growth process. From Fig. 2, during the growth process of CdSe QDs, except at the very beginning, the concentration of QDs can be regarded as a constant, as reported in some former works [16, 20]. The population density N_0 calculated from Fig. 2 was 3.92×10^{16} no./cm^3. In our reaction, the selenium concentration was excessive so that the concentration of cadmium in solution changed significantly. We can describe the particle growth in terms of cadmium concentration. The bulk solute concentration in terms of cadmium in solution C_{Cd}^b during the growth process is given by

$$C_{Cd}^b = C_{Cd}^0 - \frac{4\pi N_0 r^3}{3V_m} \tag{7}$$

where C_{Cd}^0 is the initial cadmium concentration.

Substituting Eq. (7) with Eq. (6) gives

$$\frac{\mathrm{d}r}{\mathrm{d}t} = \frac{DkV_m}{D+kr}\left(C_{Cd}^0 - C_{Cd}^{eq} - \frac{4\pi N_0 r^3}{3V_m}\right) = \frac{Dk}{D+kr}(a^3 - b^3 r^3) \tag{8}$$

where $a^3 = V_m(C_{Cd}^0 - C_{Cd}^{eq})$, $b^3 = 4/3\pi N_0$ and C_{Cd}^{eq} is the equilibrium concentration of cadmium. Xie et al. [16] estimated that C_{Cd}^{eq} contributes much less than $4/3\pi N_0$, so we treat C_{Cd}^{eq} as a constant here.

Integrating Eq. (8) yields time as a function of the radius,

$$t = \frac{1}{6Dka^2b^2}[(ak+bD)\ln\frac{a^2+abr+b^2r^2}{(a-br)^2} - 2\sqrt{3}(ak-bD)\arctan\frac{a+2br}{\sqrt{3}a}] + C \tag{9}$$

When the surface reaction process controls the overall rate of growth, Eq. (9) can be reduced to

$$t = \frac{1}{6ka^2b}\left[\ln\frac{a^2+abr+b^2r^2}{(a-br)^2} + 2\sqrt{3}\arctan\frac{a+2br}{\sqrt{3}a}\right] + C \tag{10}$$

Eq. (10) has the same form as that deduced by Bullen et al. [17] based on the surface reaction-controlled model.

On the other hand, if the diffusion process controls the overall rate of growth, Eq. (9) is reduced to

$$t = \frac{1}{6Dab^2}\left[\ln\frac{a^2+abr+b^2r^2}{(a-br)^2} - 2\sqrt{3}\arctan\frac{a+2br}{\sqrt{3}a}\right] + C \tag{11}$$

Eq. (11) has the same form as that developed by Xie et al. [16] based on the diffusion-controlled model.

Figure 5 represents the results of fitting Eq. (9) to experimental data. Two different curves, marked as curve 1 and curve 2, were fitted. The fitted values of parameters in Eq. (9) are:

$D_1 = 2.54 \times 10^{-18}$ m^2/s, $k_1 = 4.64 \times 10^{-6}$m/s,
$a_1 = 0.0734$, $b_1 = 5.06 \times 10^7$ m^{-1};
$D_2 = 9.10 \times 10^{-18}$ m^2/s, $k_2 = 7.97 \times 10^{-9}$m/s,
$a_2 = 0.0404$, $b_2 = 3.25 \times 10^7$ m^{-1}.

From Eq. (8), the maximum radius of QDs during the growth process is given as $r_{\max.} = a_2/b_2 = 1.24$ nm, which is very close to the experimental result. Two different

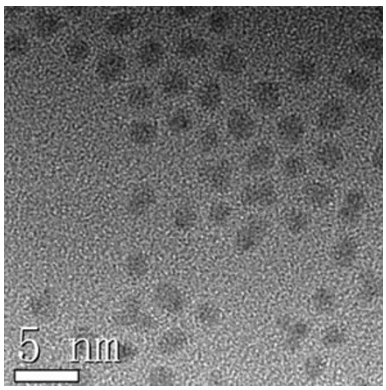

Fig. 4 High-resolution transmission electron microscopy (TEM) images of CdSe QDs

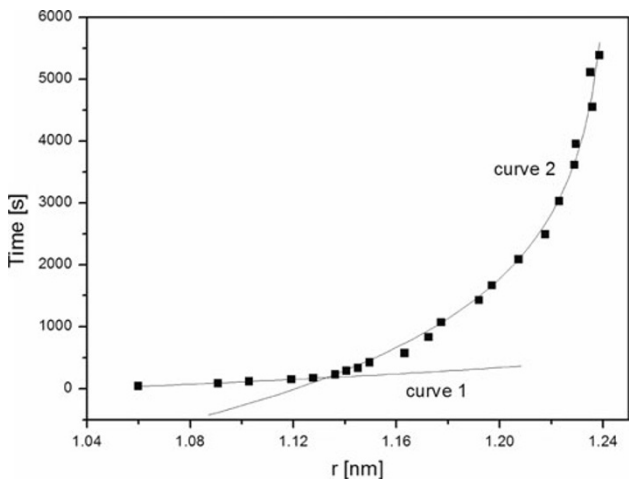

Fig. 5 Temporal evolution of the radii of CdSe QDs during synthesis and the fitting curve using Eq. (9)

fitting stages mean the growth of CdSe QDs follows different mechanisms. Because the radius was kept at the same magnitude, and using the average radius during the two growth stages, we obtained $H_1 = 0.00049$ and $H_2 = 0.95$. Hence, during the first growth stage, bulk diffusion was estimated to be more important, whereas, neither the bulk diffusion process nor the surface reaction process can be neglected during the later stage. We have discussed previously that there were some narrowing and broadening of the size distribution of CdSe QDs during the growth process. On the premise of the fitting results, the experimental change of size distribution of CdSe QDs matches well with crystallization theories. According to classic theories, at high supersaturation, the Gibbs–Thomson effect is weak, and crystal growth is usually dominated by the bulk diffusion process in which small crystals grow at a higher rate than large ones so that the particle size distribution is focused [13, 21, 22]. Sugimoto showed broadening of distribution of colloidal particles takes place all the time in the surface reaction-controlled growth due to the Gibbs–Thomson effect [23]. The fitting results show the influence of surface reaction in the second stage of growth of CdSe QDs cannot be neglected, so some broadening of distribution occurred.

Ostwald Ripening

When Ostwald ripening happened, the particle size distribution broadened quickly. The solubility difference between small particles and large ones due to Gibbs–Thomson effect became distinct. It is difficult to simulate the ensemble of QDs by Eq. (6). Therefore, the LSW theory, a rigorous mathematical approach to Ostwald ripening developed by Lifshitz and Slyozov [24] and Wagner [25], was used. For a system of highly dispersed particles, the rate law is given by

$$\bar{r}^3 - \bar{r}_0^3 = Kt \tag{12}$$

where $\bar{r}$ is the mean particle radius, $\bar{r}_0$ is the initial particle radius and K is the ripening parameter.

The results of fitting the LSW model to our experimental data are shown in Fig. 6.

The curve fitting gives satisfactory precision with a related coefficient of 0.997. The parameter values are $K = 8.32 \times 10^{-5}$ nm^3/s and $\bar{r}_0 = 1.26$ nm, which is very close to the radius maximum during the growth process.

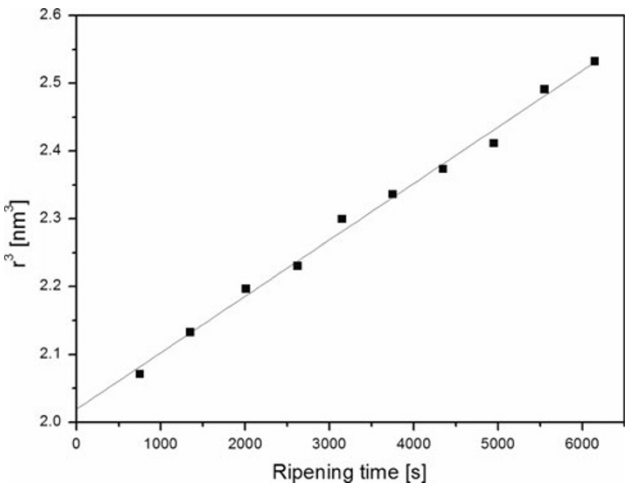

Fig. 6 Cubic of the CdSe QDs radius versus Ostwald ripening time and the fitting curve using LSW theories

Conclusions

A new model which involves both bulk diffusion process and surface reaction process was developed. When the developed model is employed, there is no need to hypothesise possible determining process. Conversely, the relative magnitude of contributions from the two processes could be indicated from the model. Using this model, the growth process of CdSe QDs was simulated, and two different growth stages were demonstrated. During the first stage, the growth of CdSe was dominated by bulk diffusion process, whereas, both processes markedly influenced the kinetics of crystal growth during the latter growth stage. At last, we successfully modelled the Ostwald ripening of CdSe QDs with LSW theories.

References

1. C.B. Murray, D.J. Norris, M.G. Bawendi, J. Am. Chem. Soc. **115**, 8706 (1993)
2. J.J. Li, Y.A. Wang, W. Guo, J.C. Keay, T.D. Mishima, M.B. Johnson, X. Peng, J. Am. Chem. Soc. **125**, 12567 (2003)
3. L. Qu, Z.A. Peng, X. Peng, Nano Lett. **1**, 333 (2001)
4. D.V. Talapin, A.L. Rogach, A. Kornowski, M. Haase, H. Weller, Nano Lett. **1**, 207 (2001)
5. O.I. Micic, C.J. Curtis, K.M. Jones, J.R. Sprague, A.J. Nozik, J. Phys. Chem. **98**, 4966 (1994)
6. A.A. Guzelian, U. Banin, A.V. Kadavanich, X. Peng, A.P. Alivisatos, Appl. Phys. Lett. **69**, 1432 (1996)
7. S.S. Kher, R.L. Wells, Nanostruct. Mater. **7**, 591 (1996)
8. N. Tessler, V. Medvedev, M. Kazes, S. Kan, U. Banin, Science **295**, 1506 (2002)
9. Z. Tan, F. Zhang, T. Zhu, J. Xu, A.Y. Wang, J.D. Dixon, N. Li, Q. Zhang, S.E. Mohney, J. Ruzyllo, Nano Lett. **7**, 3803 (2007)
10. M. Bruchez Jr, M. Moronne, P. Gin, S. Weiss, A.P. Alivisatos, Science **281**, 2013 (1998)
11. W.C.W. Chan, S. Nie, Science **281**, 2016 (1998)

12. D.V. Talapin, S.K. Poznyak, N.P. Gaponik, A.L. Rogach, A. Eychmuller, Phys. E Low-Dimension. Syst. Nanostruct. **14**, 237 (2002)
13. D.V. Talapin, A.L. Rogach, M. Haase, H. Weller, J. Phys. Chem. B **105**, 12278 (2001)
14. W.W. Yu, L. Qu, W. Guo, X. Peng, Chem. Mater. **15**, 2854 (2003)
15. X. Peng, J. Wickham, A.P. Alivisatos, J. Am. Chem. Soc. **120**, 5343 (1998)
16. C. Xie, H. Hao, W. Chen, J. Wang, J. Cryst. Growth **310**, 3504 (2008)
17. C.R. Bullen, P. Mulvaney, Nano Lett. **4**, 2303 (2004)
18. A.S. Myerson, *Handbook of Industrial Crystallization* (Butterworth-Heinemann, Boston, 2002)
19. Z.A. Peng, X. Peng, J. Am. Chem. Soc. **124**, 3343 (2002)
20. B. Pan, R. He, F. Gao, D. Cui, Y. Zhang, J. Cryst. Growth **286**, 318 (2006)
21. J.S. Wey, R.W. Strong, Photogr. Sci. Eng. **21**, 248 (1977)
22. H. Reiss, J. Chem. Phys. **19**, 482 (1951)
23. T. Sugimoto, Adv. Colloid Interface Sci. **28**, 65 (1987)
24. I.M. Lifshitz, V.V. Slyozov, J. Phys. Chem. Solids **19**, 35 (1961)
25. A.J. Ardell, R.B. Nicholson, J. Phys. Chem. Solids **27**, 1793 (1966)